Preparation, Characterization and Performances of Photocatalytic TiO$_2$-Ag$_2$O/PESf Membrane for Methylene Blue Removal

Z. Rajis, N.F.A.N. Azmi, S.N.N.M. Makhtar, M.N.A.M Norddin[*] & A. Mustafa

School of Chemical Engineering, Universiti Teknologi Malaysia,
81310 UTM Johor Bahru, Johor, Malaysia

ABSTRACT

This study proposed an effective method of methylene blue (MB) removal using a membrane with photocatalytic properties. The photocatalytic membrane, made of polyethersulfone (PESf) was incorporated with titanium dioxide (TiO$_2$) and silver oxide (Ag$_2$O) as the photocatalyst during the phase inversion process. TiO$_2$ was synthesized using sol-gel method before being modified by Ag$_2$O via wet pre-deposition method. The PESf/TiO$_2$/Ag$_2$O (PTA) membrane was characterized using scanning electron microscope coupled with elementary dispersion X-ray (SEM-EDX), X-ray diffraction analysis (XRD), attenuated Fourier transform infrared (ATR-FTIR), and ultraviolet visible near infrared (UV-vis NIR). The PTA membrane with 0.2 wt.% loading of TiO$_2$/Ag$_2$O shows uniform distribution of the photocatalyst materials and exhibits the highest degradation of MB at 85%. The TiO$_2$/Ag$_2$O presence was confirmed by the crystallinity analysis using XRD. UV-Vis NIR revealed that the band gap of TiO$_2$ reduced from 3.2 to 2.1 eV when modified with Ag$_2$O. This proved that membrane separation assisted with photocatalytic degradation is able to perform high degradation of MB dyes and has potential to be applied in industrial application.

Keywords: TiO$_2$/Ag$_2$O, PTA membrane, photocatalytic degradation, methylene blue

1.0 INTRODUCTION

Wastewater discharge contains various chemicals, grease, volatile organic compounds (VOCs), total dissolved suspended solid (TDSS) and dyes. Dyes waste can be categorized into toxic or non-toxic, water-soluble or insoluble and naturals or synthetics [1-3]. It comprises of auxochromes and chromophores, which is responsible for the colours of the dyes itself, water-solubility and the ability of the colours endurance [2]. The general purposes of dyes is solely for attraction, however dyes could bring danger as dyes are toxic, exhibits high chemical oxygen demand (COD) and might be carcinogenic and mutagenic. Dyes are difficult to be degraded as it possessed high chemical stability to withstand the colours. Despite the disadvantaged of dyes, dyes can be useful in research field especially for stain purposes or detection and to study the rate of dyes degradation [1].

Methylene Blue (MB) or methylthionininum chloride, is one of cationic dyes and was chosen as a pollutant in this study, as MB is most commonly used as substance for dyes, whether in research field or garments. MB can cause harm in the body system such as can cause eye burns, difficulty in breathing, burning sensation, nausea, vomiting, profuse sweating, mental confusion and methemoglobinemia that may lead to a permanent injury to human and animals when directly exposed to the bodies [4-6]. These dyes were typically removed using physical techniques such

as adsorption on activated carbon, coagulation by chemical agents, and ion exchange on synthetic adsorbent resins. However, these techniques are only able to change the organic compounds from liquid to solid state which contributes to secondary pollution and required a high cost to regenerate the adsorbent materials [7-9]. Due to these reasons, photocatalytic degradation is one of a best choice to treat dyes wastewater especially in degrading persistent chemical compounds such as azo dyes into harmless simple compounds.

Photocatalysis using titanium dioxide (TiO_2) as catalysts one of the most widely used methods in wastewater treatment. The catalyst is irradiated with light sources, i.e., solar light and UV light with the presence of pollutants. The light sources bombard the catalyst and excite the electrons, causing it to degrade the pollutants into more simpler and harmless products. These products then can be released into open water bodies.

TiO_2 is a well-known semi-conductor photocatalyst, with good oxidizing aptitude, low cost, low toxicity, stable thermally and chemically, specifically in photoelectron chemical (PEC) application. Regardless of all the advantages, TiO_2 has a wide band gap of about 3.2 eV, which is in the ultraviolet region, with the range of wavelength less than 300 nm. For TiO_2 to absorb visible light, it needs to be in the visible range, that is 300 nm $< \lambda <$ 390 nm and energy below 3.0 eV. For this reason, TiO_2 has been modified to lower its band gap to fit in the visible light range.

The modification of TiO_2 is generally done either by doping or surface modification. Doping, or combine modification is the simplest way, as it combined two or more photocatalyst material/s. It is interesting to combine Ag_2O with TiO_2 as a doping modification technique to lower TiO_2 band gap energy.

Despite of all advantages of combine TiO_2 and Ag_2O such shows highest removal of pollutant, there also have some limitation on photocatalyst recovery issue at the end of the treatment process [10]. Thus, it is worth to blend catalyst with polymer membrane which acts as a host since it has an outstanding mechanical strength, thermal stability, film forming stability and dual function of materials with filtration and photocatalyst activities. In addition, this combination can produce cleaner permeate and the membrane used can promote the regeneration of catalyst [11-12]. In addition, there is no previous studies which blend in TiO_2 and Ag_2O in PESf membrane [13].

Therefore, in this paper, photocatalytic (PTA) membrane was prepared by combining TiO_2 with Ag_2O through doping technique and incorporated in polyethersulfone (PESf). The ratio of TiO_2/Ag_2O was varied to 0.1, 0.2, 0.3 and 0.5 by weight percent into the PESf membrane. The PTA membranes were characterized using scanning electron microscope (SEM) coupled with elementary dispersion x-ray (EDX), fourier transform infrared (FTIR) and ultraviolet visible near infrared (UV-Vis-NIR). TiO_2/Ag_2O was characterized using x-ray diffraction (XRD) for crystallinity study. Finally, the performance of PTA membranes was examined by the photocatalytic degradation of MB dye.

2.0 METHODS

2.1 Materials

Chemicals used in this study consisted of titanium butoxide (Ti(OBu4)) and silver nitrate ($AgNO_3$) as a precursor for TiO_2,and Ag_2O, respectively. Nitric acid (HNO_3) with 65% purity, isopropanol (C_3H_8O) with 99% purity was used to synthesize TiO_2. Sodium hydroxide (NaOH) was used to synthesize Ag_2O solution. N-Methyl-2-pyrrolidone (NMP) was used as solvent for PESf dope and polyvinylpyrrolidone (PVP) was used as

pore former. The solution was prepared using distilled water was used throughout the study. All the chemicals were purchased from Sigma Aldrich and used as received without further purification

2.2 Preparation of Photocatalyst TiO₂/Ag₂O

TiO_2 was prepared using a sol gel method based on the procedure from the previous study [14]. The $Ti(OBu_4)$ was used as TiO_2, which formed under two processes, hydrolysis and peptidzation First, 25 mL of $Ti(OBu_4)$ was added dropwise into 8 mL of isopropanol solution. The solution was stirred continuously until the mixture was homogenous. After that, 200 mL of distilled water was dropwise to initiate the hydrolyzation process. The mixture was stirred for 30 minutes using a magnetic stirrer. Next, 3 mL of HNO_3 was added into the solution and stirred vigorously for another 30 minutes.

The prepared mixture was then transferred to an air-tight container and aged until a yellowish sol–gel was formed. The gel was dried in a vacuum oven at 75°C for 74 hours until a yellowish powder was observed. Finally, the powder was calcined at 400°C for 2 hours. The resultant powder was washed using distilled water and isopropanol for several times and dried at 60°C for 24 hours. About 40 mg of obtained TiO_2 powder was dispersed in 80 mL of distilled water with 29 mg of $AgNO_3$ and stirred vigorously for 10 minutes. The Ag_2O was synthesized by adding 20 mL of 0.05 M NaOH dropwise into the solution. After that, the solution was further stirred for another 30 minutes to promote dispersion of Ag_2O on TiO_2 surface. After 30 minutes, black-greyish powder was formed at the bottom of the solution. The powder were filtered and washed for few times using distilled water and ethanol to remove impurities. Finally, they were dried in a vacuum oven at 60°C for 12 hours [14].

2.3 Fabrication of TiO₂/Ag₂O with PESf

The powder of TiO_2/Ag_2O was dispersed in NMP solvent for 3 hours, before added the PESf and PVP and stirred for 24 hours 350 rpm under 50 °C temperatures for 24 hours. The loading of TiO_2/Ag_2O was varied into 4 loadings, which were 0.1%, 0.2%, 0.3% and 0.5%. The dope solution was then casted on glass plate and quickly immersed in a distilled water bath at 15-1°C. The phase inversion membrane was later transferred to fresh distilled water for 24 hours to complete the solidification process and to remove the excess solvent on the membrane. Finally, the membrane was air dried for 24 hours [14]. The composition of PTA membranes is shown in Table 1.

Table 1 Composition of PESf with different loading of TiO₂/Ag₂O

Membrane	PESf (%)	PVP (%)	TiO₂/Ag₂O (%)
PTA 0.1	27	5	0.1
PTA 0.2	27	5	0.2
PTA 0.3	27	5	0.3
PTA 0.5	27	5	0.5

2.4 Characterization

The morphology of PTA membrane was examined using scanning electron microscope (SEM) combined with energy dispersive x-ray (EDX) (JEOL JSM-IT300LV, JAPAN). The sample was immersed in liquid nitrogen for several minutes and let it fracture spontaneously for the membranes cross section. Samples were then coated with gold under vacuum for 5 min for the crystallinity study of TiO_2, Ag_2O and combination of TiO_2/Ag_2O, the sample was analyzed using x-ray diffraction analysis (XRD, RIGAKU) within range of 20° to 80° to confirm that the heterojunction photocatalyst consisted of TiO_2 and

Ag_2O. The crystallite size was determined using the Scherrer's equation as follows:

$$D = K \lambda / \beta \cos\theta \tag{1}$$

where K is the Scherrer constant, $\lambda = 0.15406$ nm is the X-ray wavelength, β is the peak width of half-maximum, and θ is the Bragg diffraction angle.

The formation of the synthesized TiO_2's containing anatase and rutile was calculated using equation 2:

$$X_A = 100/(1 + 1.265 I_R/I_A) \tag{2}$$

where X_A is the weight fraction of anatase in the mixture, I_A is the intensity of anatase diffraction and I_R is the intensity of rutile diffraction [15].

The chemical compositions of PESf and PTA membrane were determined using attenuated total reflection Fourier transform infrared (ATR-FTIR) (Nicolet Magna-IR560) in the range between 650-4000 cm^{-1}. The band gap of the PESf and PTA membranes were analyzed using UV-Vis NIR Spectrophotometer within ranging from 220 to 600 nm. For comparison purposes, the PESf blended with neat TiO_2 (PT) membrane and PESf blended with neat Ag_2O (PA) membrane were also cast and tested. The data collected from the UV-Vis NIR was used in the Planck's equation 3 as follows:

$$E = h\nu/\lambda \tag{3}$$

where E is the energy (in Joules), h is the Planck constant (6.63 x 10-34), v is the frequency (s^{-1}) and λ is the wavelength (nm).

2.5 Photocatalytic Activity of the Membrane

The band gap of TiO_2 and Ag_2O were studied using ultraviolet visible spectrophotometer (UV-Vis spectrometer). The photocatalytic degradation was performed on methylene blue (MB) in a photoreactor. The samples were weight 0.1g and cut into 1cm x 1cm dimension. The samples were immersed in 5 ppm MB solution and placed in UV Vis reactor. The lamp was positioned 10 cm above the filtration cell. The UV Vis light was obtained from an ultraviolet (UV) lamp (Vilber Laurmat, France, VL-115-M, ʎ = 312 nm, 30 W, with light intensity of 1.45 mW/cm^2). The visible light was obtained white light-emitting diode (LED) flood light (Wuhan Co-Shine Technology Co., Ltd China, CS-FL, ʎ > 420 nm, 30 W, light intensity of 96 mW/cm^2.

The removal of MB solution was determined by calculating the concentration of the MB solution during the photocatalytic process. The sample of Mb solution was taken every 30 minutes interval for 4 hours. The solutions were placed in UV-Vis spectrophotometer Dr 5000 to calculate the concentration left in the sample. The percentage of MB removal (d %) was calculated using the following equation [1]:

$$\% \text{ Removal} = \frac{C_o - C_t}{C_o} \times 100 \tag{4}$$

where C_o is absorbance at t = 0 minute and C_t is absorbance at t minute.

3.0 RESULTS AND DISCUSSION

3.1 Surface Analysis of PTA Membranes

The PTA's membranes surface and cross section morphology were investigated using SEM as showed in Figure 1. This study was done to examine the effect of TiO_2/Ag_2O modification on neat PESf membrane through SEM images and the distribution of TiO_2/Ag_2O particles on the membranes.

Figure 1a(i) is the neat PESf membrane surface image while Figure 1b-e(i) is the images PTA membranes. The surface of

the PESf membrane is almost the same as the previous studies, where the surface is smooth and the pores are hardly seen [17-19]. On the other hand, the distribution of TiO$_2$/Ag$_2$O catalyst can be clearly seen on the surface of the membranes distinguish by the white dots on the surface. The addition of TiO$_2$/Ag$_2$O makes the surface looks rougher, which indicates the presence of the heterojunction catalyst. The rough distribution of the catalyst is increased as its weight loading is increased up to 0.2 wt % but suddenly becomes smoother as the loading exceeded 0.3 wt % to 0.5 wt %. This is probably due to the catalyst being embedded in the outer surface of the membrane.

The surface roughness is essential for the photo degradation of MB solution as the photo degradation of the membrane take place on the surface. This was proved with the PTA's membranes performances 0.1 wt. % and 0.2 wt. % of TiO$_2$/Ag$_2$O with the rough surface showed better performances compared to neat PESf and PTA membranes with 0.3 wt. % and 0.5 wt. % of TiO$_2$/Ag$_2$O.

Figure 1a(ii) shows the cross section of the PTA's membrane with neat PESf as the controlled, Figure 1 b-e(ii) as the PTA's membrane, and modified PESf membrane with TiO$_2$/Ag$_2$O loading. Generally, the membranes exhibited two layers, which are dense skin layer on top and finger-like structure at the bottom. These structures were produced due to the phase inversion during the fabrication of the membranes [17, 20].

Generally, the PTA membranes thickness increased as the catalyst loading increased. This is due to the fact that the catalyst is embedded onto the outer membrane surface. However, according to the image analysis software, membrane changed roughly in the order of c>d>a>e>d. Based on the surface analysis, the diameter of TiO$_2$ and Ag$_2$O were estimated between 20.25 nm-56.04 nm and 9.54 nm – 12.56 nm, respectively.

Meanwhile, thickness of casting solution is 0.5 mm. Thus, the thinner membranes are more preferable to achieve the highest MB removal. Therefore, PTA membrane with 0.1 wt. % and 0.2 wt. % TiO$_2$/Ag$_2$O produce better membrane performance.

Figure 2(b-e) shows EDX images of PTA membranes surface. The image shows the neat PESf with different weight loading of 0.1 wt. %, 0.2 wt. %, 0.3 wt. % and 0.5 wt. % of the TiO$_2$/Ag$_2$O catalyst. Approximately 0.1 % and 2.03 % percentage of titanium and argentum respectively were found in the PTA's membrane. The low percentage of titanium and argentum was due to nanoparticles leached out when the membrane was immersed into the water bath during the phase inversion process [2-3, 21-22].

The crystallinity of TiO$_2$, Ag$_2$O and combined TiO$_2$/Ag$_2$O photocatalyst was examined using XRD analysis as shown in Figure 3. It was found that the obtained TiO$_2$ from the sol-gel synthesized consists of 83.84 % anatase and 16.16 % rutile crystal phase, where the mixture of anatase and rutile would increase the photo degradation effect [16]. The anatase peaks of TiO$_2$ can be observed at 28º, 48º, and 69º while rutile peaks are at 29º, 36º, and 43º as detected in International central for diffraction data (ICDD) database. On the other hand, Ag$_2$O peaks can be observed at 32º, 38º, 43º and 63º. The TiO$_2$/Ag$_2$O crystallinity phase showed combine peaks of TiO2/Ag$_2$O, which confirmed the successfully synthesized of TiO$_2$/Ag$_2$O heterojunction photocatalyst. FTIR analysis was used to further verify the present of TiO$_2$/Ag$_2$O in the sample.
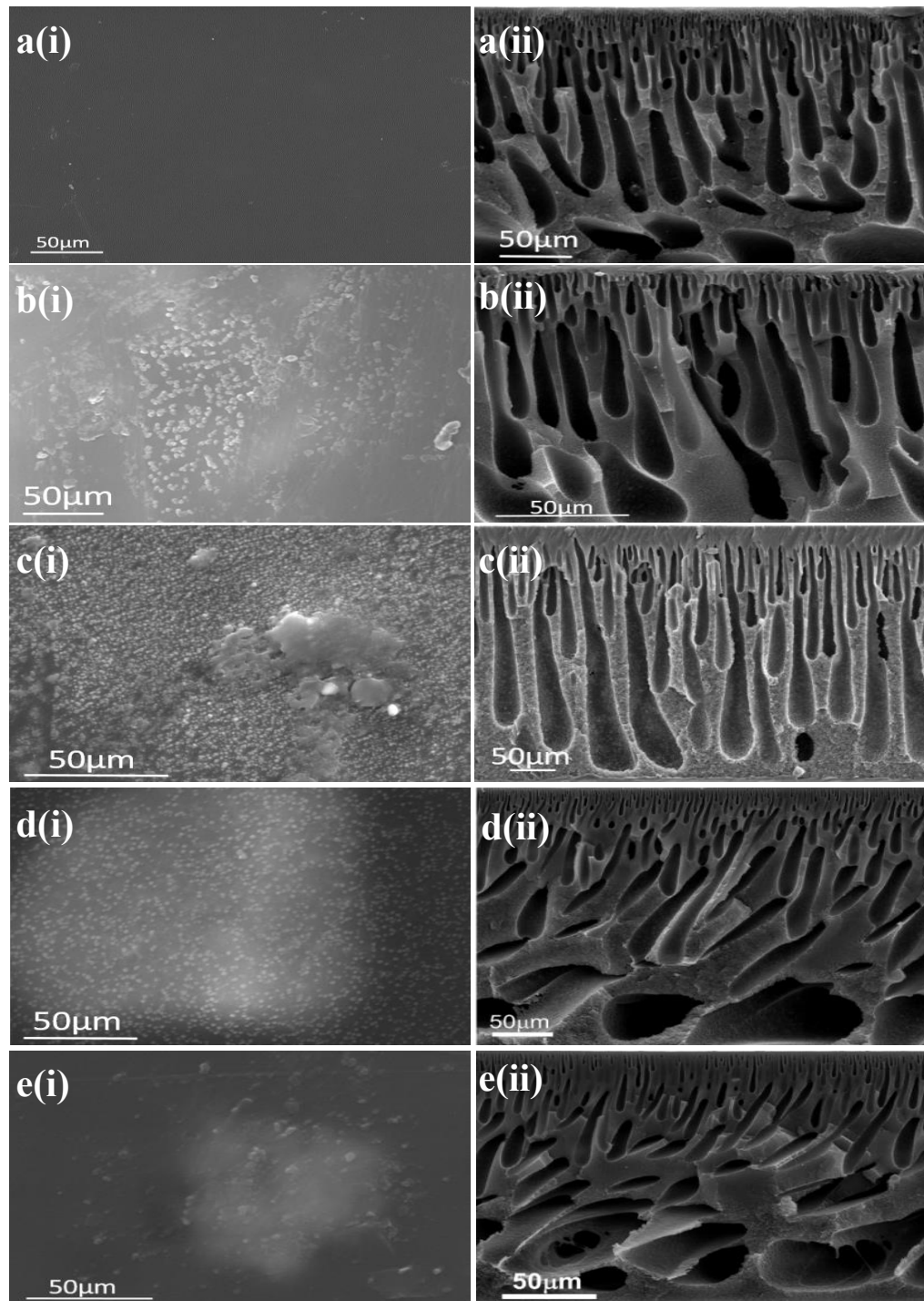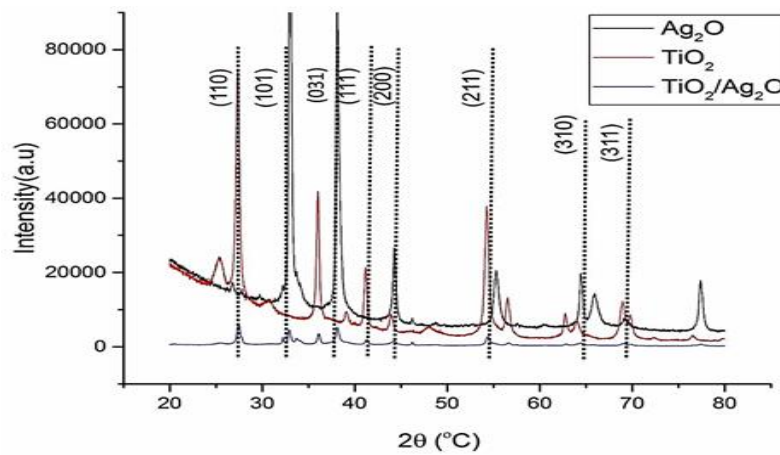
Figure 1 SEM images for the (i) membrane surface (ii) cross section of (a) neat PESf, (b) 0.1 wt. %, (c) 0.2 wt. %, (d) 0.3 wt. % and (e) 0.5 wt. % of the TiO$_2$/Ag$_2$O PTA's membranes
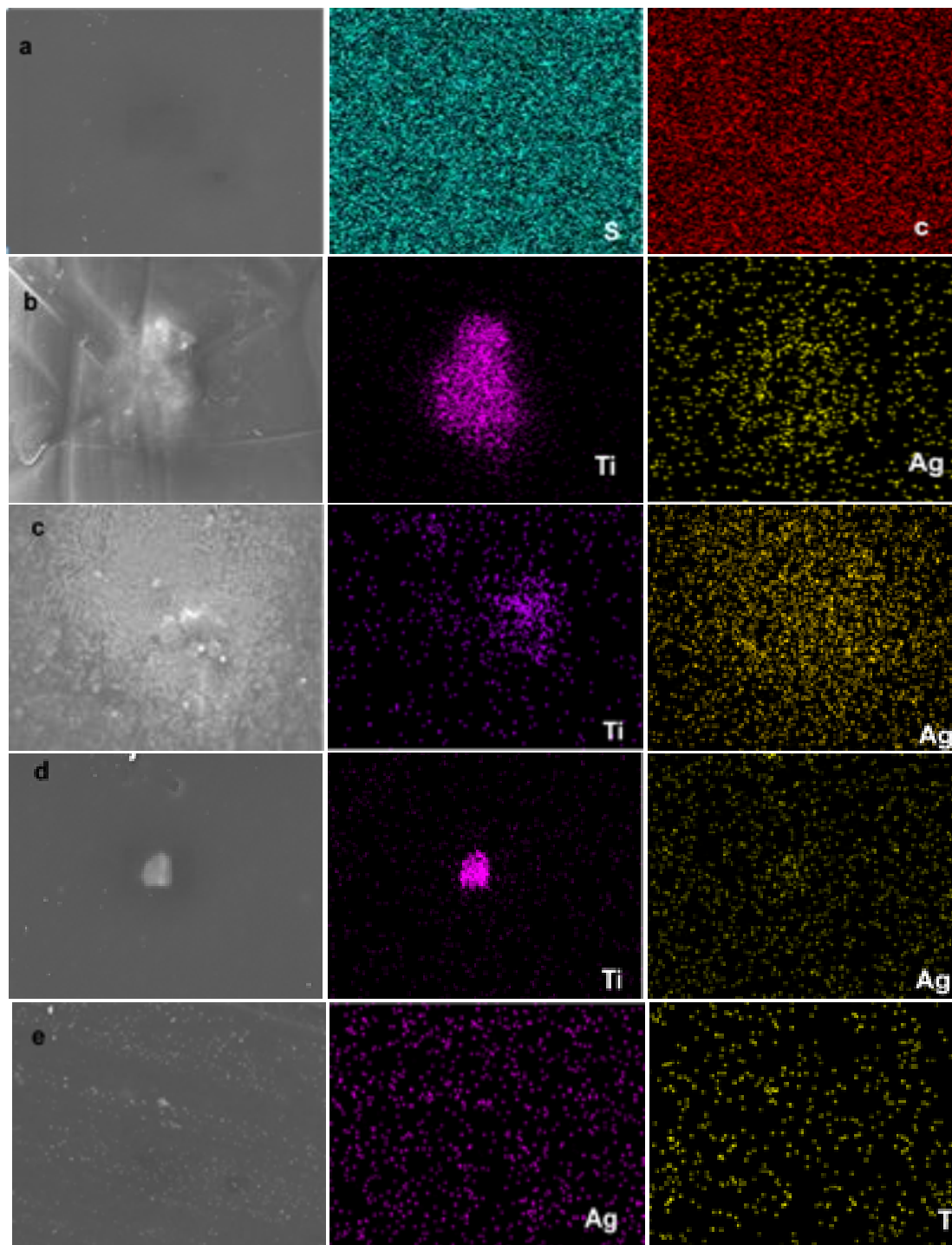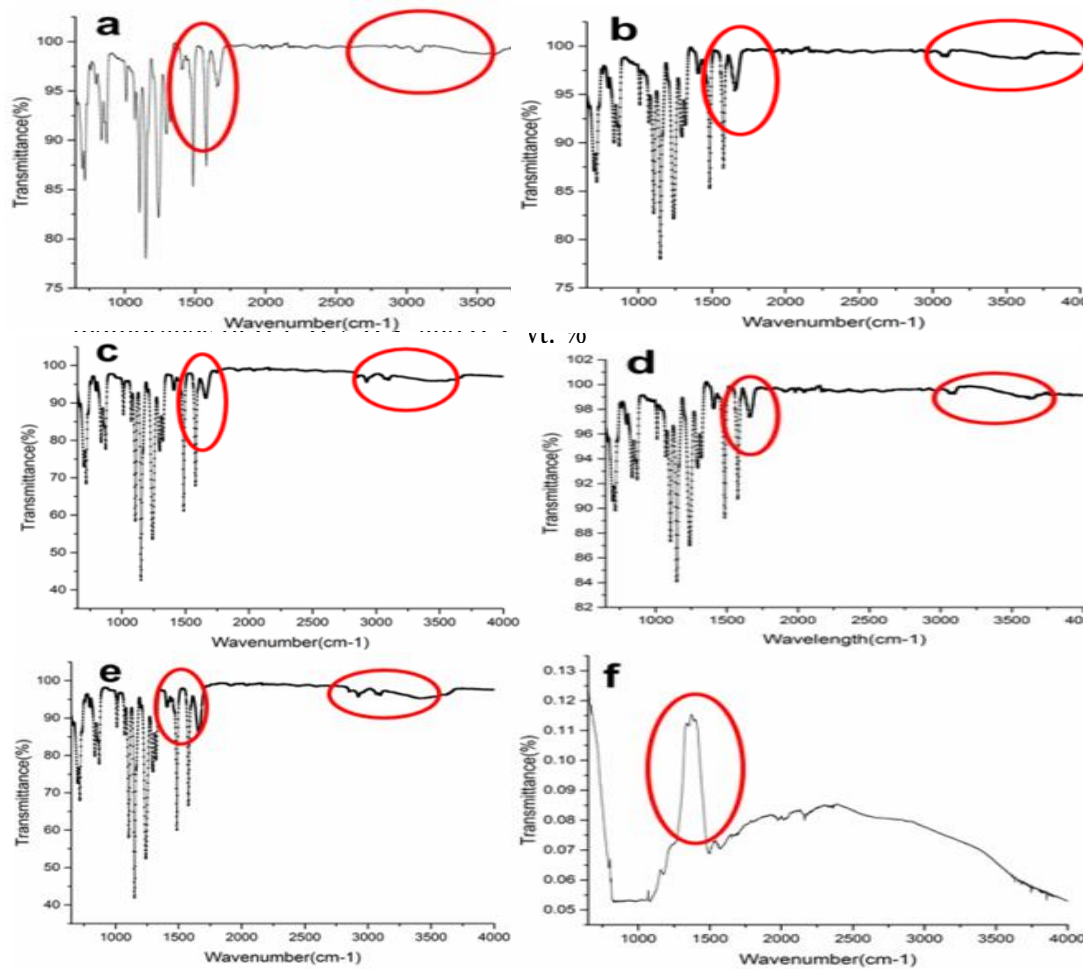
Figure 2 EDX images for the membrane surface of (a) neat PESF, (b) 0.1 wt. %, (c), 0.2 wt. % (d) 0.3 wt. % and (e) 0.5 wt. % of the TiO$_2$/Ag$_2$O PTA's membranes

Figure 3 XRD patterns for TiO$_2$, Ag$_2$O and TiO$_2$/ Ag$_2$O

Figure 4 FTIR spectra for PESf and PTA membranes (a) neat PESf (b) 0.1 wt. %, (c) 0.2 wt. %, (d) 0.3 wt. %, (e) 0.5 wt. % of PTA membranes and (f) TiO$_2$/Ag$_2$O

The chemical compositions of the PTA membranes were studied using FTIR-ATR under as presented in Figure 4. The figure illustrate the neat PESf and PTA membranes of 0.1, 0.2, 0.3, and 0.5 wt. % TiO_2/Ag_2O photocatalyst. The PTA's membranes exhibited almost identical spectra as neat PESf membrane. No TiO_2/Ag_2O peak was observed in the PTA's membrane because of the low loading of TiO_2/Ag_2O catalyst in the membrane. S = O symmetric stretch peaks can be observed at 1150 cm-1 and 1307 cm^{-1}, CSO_2C asymmetric stretch is around 1322 cm^{-1}, C-O asymmetric stretch on 1244 cm^{-1} and 1000 cm^{-1} [23-24]. C_6H_6 ring stretch peak can be seen at 1590 cm^{-1}, O-H aliphatic and aromatic stretch peaks are at 2886 cm^{-1} and 2940 cm^{-1}, respectively. TiO_2/Ag_2O peak can be observed in Figure 4(f) approximately around 1500 cm^{-1}. The range showed between 1200-1800 nm and 2900-3800 nm exhibit slight different peaks, despite the low addition of TiO_2/Ag_2O. These results also supported and confirmed the existence of the TiO_2/Ag_2O heterojunction photocatalyst in the membrane PESf membranes.

3.2 Photocatalytic Activity

The band gaps of PTA membranes were determined using a UV-Vis NIR Spectrophotometer. The band gap reduces according to the incorporation of TiO_2/Ag_2O into PESf membrane. The data obtained from the Planck equation is plotted in a graph as shown in Figure 5 and Figure 6. The data was split into two graphs due to different intensities of the data. From the graph, the band gap values of the membranes are determined by extrapolating the curve to cross the X-axis. The band gap values are summarized in Table 2.

From the results, the PA membrane shows the lowest band gap of 1.9 eV while the PT membrane shows the highest band gap of 3.0 eV and the band gap of PTA

membranes are in the middle. Based on the results obtained, it is clear that the blending of TiO_2/Ag_2O heterojunction catalysts able to reduce the band gap of PT membrane from 3.2eV to 2.1 eV. As the Ag_2O is bound with TiO_2, the excited electron from Ag particles is supplied to Ti, and indirectly reduces the wide band gap of Ti. PTA membrane with 0.2 and 0.3 wt. % TiO_2/Ag_2O have the same band gap which is 2.1 eV and PTA 0.1 wt. % and 0.5 wt. % also possesses similar band gap value which is 2.5 eV. This shows that the lowest reduction of the band gap for the modified membrane is 2.1 eV. PA membrane exhibited the lowest band gap since the band gap of Ag_2O which is 1.3 eV.

Table 2 Band gap estimation for PESf and PTA membranes

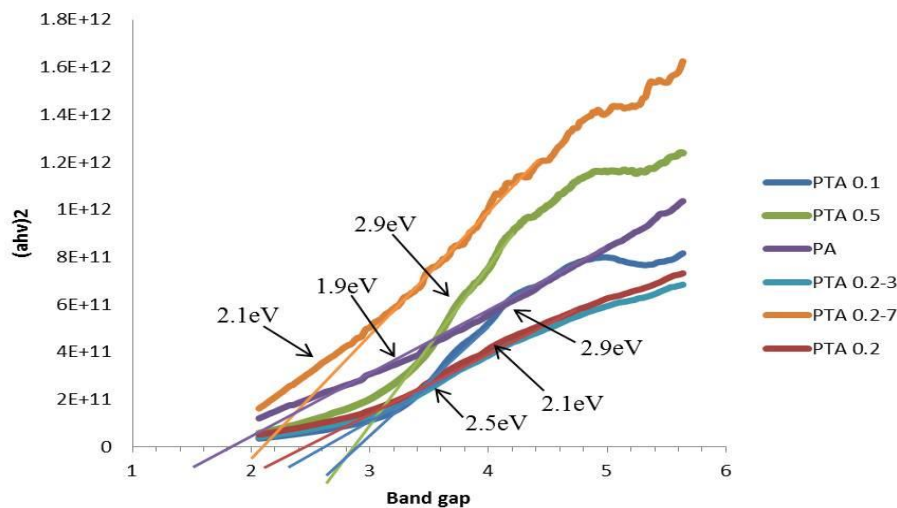| Membrane	Band gap
TiO_2 neat	3.2
PTA 0.1	2.9
PTA 0.2	2.1
PTA 0.3	2.1
PTA 0.5	2.9
PT	3.0
PA	1.9

3.2.1 MB Absorption of PTA Membranes under Dark Region

Neat PESf and PTA membranes were evaluated for photo degradation. All membranes undergo the dark absorption process as shown in Figure 7.

TiO_2/Ag_2O heterojunction photocatalyst exhibited the highest absorption at 70%, followed by neat TiO_2 at 55% and neat Ag_2O at 25% at the equilibrium state. It showed that the synthesized TiO_2/Ag_2O heterojunction photocatalyst is stable and capable of absorbing the MB better than the neat TiO_2 and Ag_2O alone. This is most probably due to the lower band gap possessed by the TiO_2/Ag_2O

heterojunction photocatalyst as compared to TiO$_2$ and Ag$_2$O. Even though the band gap of Ag$_2$O is the lowest, its absorption is not as good as TiO$_2$/Ag$_2$O because of the stability since Ag$_2$O is unstable.
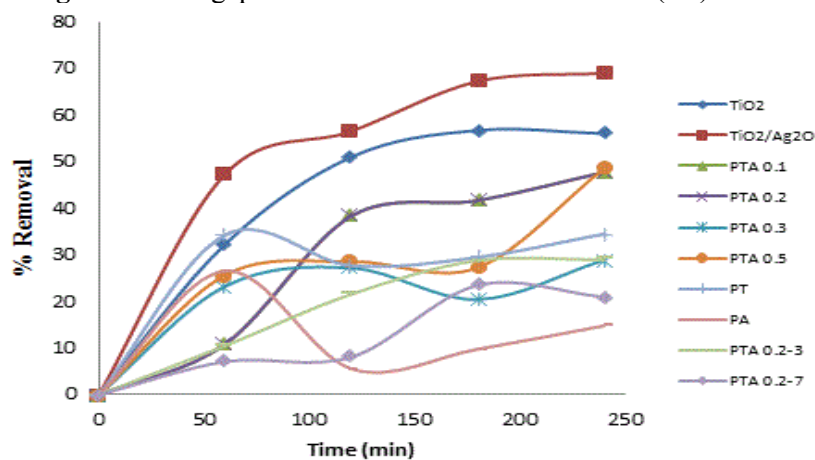
Therefore, it can be concluded that the TiO$_2$/Ag$_2$O heterojunction photocatalyst has been successfully enhanced the of MB absorption.

Figure 5 Band gap spectra for PESf blended with neat Ag2O (PA) and PTA membranes
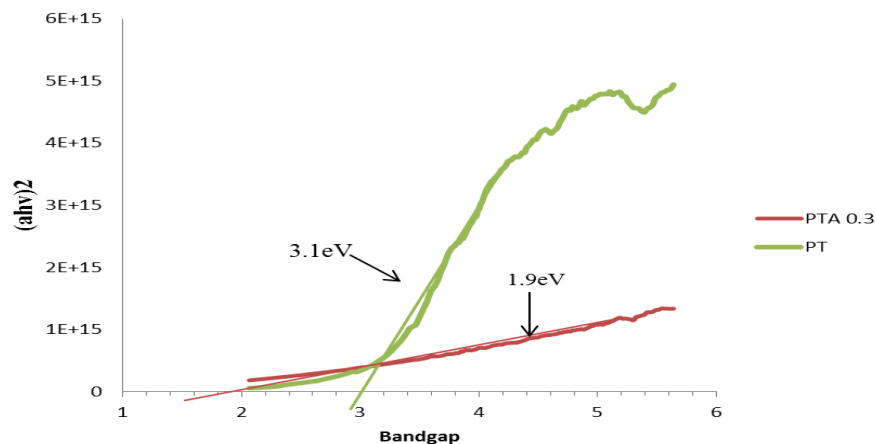
Figure 6 Band gap for PESf blended with neat TiO2 (PT) and PTA membranes

Figure 7 Absorption graph for PESf blended with neat Ag$_2$O (PA), PESf blended with neat TiO$_2$ (PT) and PTA membranes under dark region

The effect of modifying PESf membrane with the addition of TiO_2/Ag_2O (PTA), neat TiO_2 and neat Ag_2O can be seen in Figure 7. All modified membranes (PTA) show decreasing absorption values as compared to the neat catalyst (neat TiO_2 and Ag_2O) results. 0.1 and 0.2 wt. % loading of TiO_2/Ag_2O heterojunction photocatalyst produced the highest absorption result among the PTA membranes, which are about 40 %, followed by PT at 30 % and 0.3 and 0.5 wt. % loading TiO_2/Ag_2O at 20 %. The lowest value was obtained by PA which is at 10 %. These are expected as the neat catalysts are exposed more to the MB solution compared to the PTA membranes where they are embedded in the PESf membrane. Nevertheless, from this result it also can be concluded that the modified PESf membrane with TiO_2/Ag_2O heterojunction photocatalyst has enable a better MB absorption than the PT membrane. 0.1 and 0.2 wt % are better than 0.3 and 0.5 wt % in terms of the loading of the heterojunction catalyst. It is probably because a higher loading might expose more Ag_2O to the MB solution.

3.2.2 MB Photocatalytic Degradation of PTA Membranes under UV Light Region

Figure 8 shows the photocatalytic degradation for PESf blended with neat Ag_2O (PA), PESf blended with neat TiO_2 (PT) and PTA membranes under UV light region. According to the results, all modified PTA membranes are able to remove MB solution better than PT and PA. 0.2 wt. % loading of TiO_2/Ag_2O (PTA 0.2) exhibited the highest photo degradation with 85 %, followed by 0.1 wt. % loading of TiO_2/Ag_2O (PTA 0.1) with 80 % degradation. Decreasing of MB removal is due to the increasing of TiO_2/Ag_2O loading since the surface

area are reduced significantly with increased photocatalyst loading.

As the UV light illuminates Ag particles, the particles dissociate and release electrons. The electrons are then supplied to TiO_2, which then degrade the MB particles. The recombination rate of TiO_2's electron is longer and thus, many MB particles were degraded into CO_2 and H_2O [25]. Besides, the photodegradation MB process it also release some intermediate product such as 2-amino-5-(N-methyl formamide) benzene sulfonic acid, 2-amino-5-(methyl amino)-hydroxybenzene sulfonic acid, benzenesulfonic acid and phenol [26].

The PT membrane has only achieved about 34 % removal which is most probably due to its high band gap of 3.2 eV that prevented it from degrading more MB solution. As for PA membrane, it has the lowest MB removals which are only 14 %. This can be explained by the stability of the Ag_2O. Ag_2O without any combination with any other photocatalyst is not stable under UV irradiation.

Thus, PA cannot remove higher MB particles than other modified membranes. The performance of PTA membranes is higher than PT or PA membranes where the MB degradation has achieved up to 85%. In the previous studies [27-29], where PESf was modified with TiO_2 alone, the degradation result did not achieve 85%. This confirmed that the TiO_2/Ag_2O heterojunction catalyst have achieved an amazing 85 % of photocatalytic degradation even though it was used in a small quantity.

Figure 9 illustrates the photocatalytic degradation process in the MB solution with the presence of PTA membranes. During photocatalytic degradation process, MB particles absorb the light when irradiated under UV light. This excited MB particles to a singlet state and then to triplet state. On the same

time, TiO_2 and Ag_2O particles were also excite via UV irradiation, TiO_2 and Ag_2O electron were jumped to conduction band, leaving photon holes behind. The electrons are negatively charged combined with MB, which is positively charged, and reduce it a leuco form. This form was further degraded into last products, which are carbon dioxide and water. Since TiO_2 is combined with Ag_2O, the electrons from Ag_2O were directly supplied to TiO_2 and resulted in higher electron species increase the degradation rate.
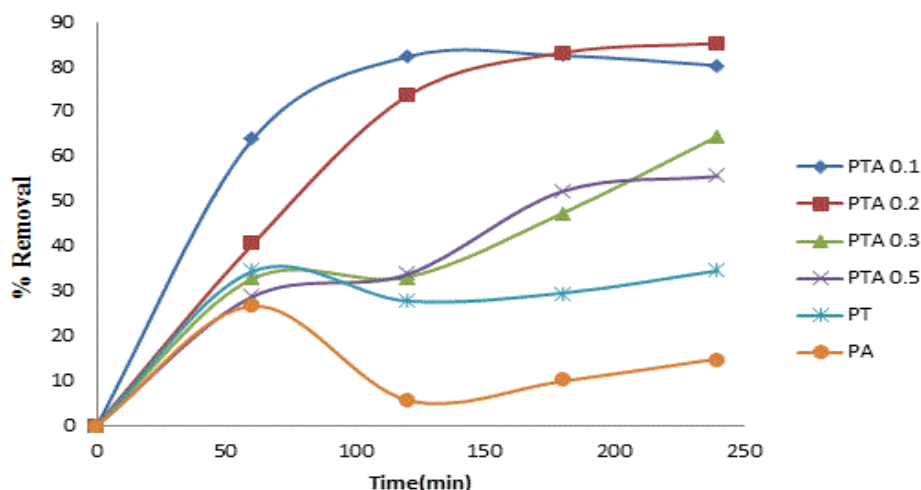
Figure 8 Photocatalytic degradation for PESf blended with neat Ag_2O (PA), PESf blended with neat TiO_2 (PT) and PTA membranes under UV region
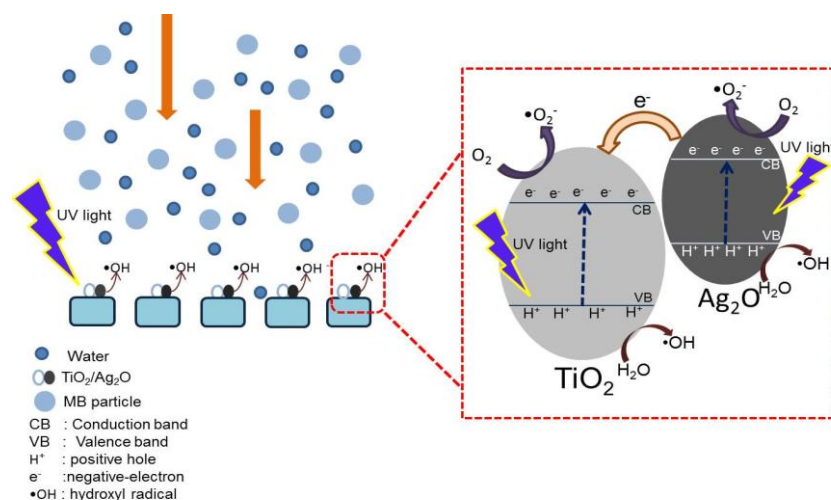
Figure 9 Schematic photocatalytic degradation process in the MB solution of PTA membrane

4.0 CONCLUSION

This study successfully synthesized photocatalyst (TiO_2, Ag_2O and TiO_2/Ag_2O) and PTA membrane ($TiO_2/Ag_2O/PESf$) via sol-gel and phase inversion method, respectively. TiO_2 and Ag_2O were embedded in PESf with 4 different loadings. Based on the results obtained, PTA with 0.2 wt. % loading of TiO_2/Ag_2O showed 85% degradation with good catalyst distribution and lower band gap than neat TiO_2. Thus, these findings show the membrane separation assisted with photocatalytic properties yield high removal of MB with a simpler method,

which is desirable used in industrial field.

ACKNOWLEDGEMENT

REFERENCES

[1] B. A. Fil, C. Özmetin, and M. Korkmaz. 2012. Cationic Dye (methylene blue) Removal from Aqueous Solution by Montmorillonite. *Bull. Korean Chem. Soc.* 33(10): 3184-3190.

[2] H. Xiao, T. Zhao, C. H. Li, and M. Y. Li. 2017. Eco-friendly Approaches for Dyeing Multiple Type of Fabrics with Cationic Reactive Dyes. *J. Clean. Prod.* 165: 1499-1507.

[3] L. Cai, T. Xu, J. Shen, and W. Xiang. 2015. Highly Efficient Photocatalytic Treatment of Mixed Dyes Wastewater via Visible-light-driven AgI – Ag$_3$PO$_4$/MWCNTs *Mater. Sci. Semicond. Process.* 37: 19-28.

[4] I. A. W. Tan, A. L. Ahmad, and B. H. Hameed. 2008. Adsorption of Basic Dye on High-surface-area Activated Carbon Prepared from Coconut Husk: Equilibrium, Kinetic and Thermodynamic Studies. *J. Hazard. Mater*. 154(1-3): 337-346.

[5] I. A. W. Tan, A. L. Ahmad, and B. H. Hameed. 2008. Adsorption of Basic Dye Using Activated Carbon Prepared from Oil Palm Shell: Batch and Fixed Bed Studies. *Desalination*. 225(1-3): 13-28.

[6] D. Ghosh and K. G. Bhattacharyya. 2002. Adsorption of Methylene Blue on Kaolinite. *Applied Clay Science*. 20: 295-300.

[7] W. A. Mcgowan. 1995. Environmental Requirements.

[8] H. Lachheb. 2002. Photocatalytic Degradation of Various Types of Dyes (Alizarin S, Crocein Orange G, Methyl Red, Congo Red, Methylene Blue) in Water by UV-Irradiated Titania. *Appl. Catal. B Environ.* 39(1): 75-90.

[9] A. Rahimpour, S. S. Madaeni, A. H. Taheri, and Y. Mansourpanah. 2008. Coupling TiO$_2$ Nanoparticles with UV Irradiation for Modification of Polyethersulfone Ultrafiltration Membranes. *J. Membr. Sci.* 313(1-2): 158-169.

[10] V. Ghaffarian, S. M. Mousavi, M. Bahreini, and H. Jalaei. 2014. Polyethersulfone/poly (butylene succinate) Membrane: Effect of Preparation Conditions on Properties and Performance. *J. Ind. Eng. Chem.* 20(4): 1359-1366.

[11] L. Shen. 2012. Preparation and Characterization of ZnO /polyethersulfone (PES) Hybrid Membranes. *Desalination*. 293: 21-29.

[12] N. Maximous, G. Nakhla, W. Wan, and K. Wong. 2009. Preparation, Characterization and Performance of Al$_2$O$_3$/PES Membrane for Wastewater Filtration. *J. Memb. Sci.* 341(1-2): 67-75.

[13] D. Jafar, Z. Yaakob, and S. Shahgaldi. 2011. Synthesis and Characterization of PES / TiO$_2$ Nanofibers Membrane. 315: 613-619.

[14] I. C. Kim, J. G. Choi, and T. M. Tak. 1999. Sulfonated Polyethersulfone by Heterogeneous Method and Its Membrane Performances. *J. Appl. Polym. Sci.* 74(8): 2046-2055

[15] Z. Rajis, A. Noorul, Mohammad Mohd, and A. Mustafa. 2017. Preparation and Structural Characterization of Binary Catalyst for Dye Wastewater. *J. Teknol.* 2: (79): 65-71.

[16] G. Wu, S. Gan, L. Cui, and Y. Xu. 2008. Effect of Polyamide Molecular Structure on the Performance of Reverse Osmosis Membrane. *Appl. Surf. Sci.* 254: 7080-7086.

[17] W.-J. Yin, S. Chen, J.-H. Yang, X.-G. Gong, Y. Yan, and S.-H. Wei. 2010. Effective Band Gap Narrowing of Anatase TiO [sub 2] by Strain Along a Soft Crystal Direction. *Appl. Phys. Lett.* 96(22): 221901.

[18] M. Z. Shahruddin, N. Zakaria, N. F. D. Junaidi, N. H. Alias, and N. H. Othman. 2016. Study of the Effectiveness of Titanium Dioxide (TiO_2) Nanoparticle in Polyethersulfone (PES) Composite Membrane for Removal of Oil in Oily Wastewater. *J. Appl. Membr. Sci. Technol.* 19: 33-42

[19] G. Couture, A. Alaaeddine, F. Boschet, and B. Ameduri. 2011. Polymeric Materials as Anion-exchange Membranes for Alkaline Fuel Cells Prog. *Polym. Sci.* 36(11): 1521-1557.

[20] E. Yuliwati, A. F. Ismail, T. Matsuura, M. A. Kassim, and M. S. Abdullah. 2011. Characterization of Surface-modified Porous PVDF Hollow Fibers for Refinery Wastewater Treatment Using Microscopic Observation. *Desalination.* 283: 206-213.

[21] A. Sotto, A. Boromand, S. Balta, J. Kim, and B. Van der Bruggen. 2011. Doping of Polyethersulfone Nanofiltration Membranes: Antifouling Effect Observed at Ultralow Concentrations of TiO2 nanoparticles. *J. Mater. Chem.* 21: 10311.

[22] A. Rahimpour and S. S. Madaeni. 2010. Improvement of Performance and Surface Properties of Nano-porous Polyethersulfone (PES) Membrane Using Hydrophilic Monomers as Additives in the Casting Solution. *J. Membr. Sci.* 360: 371-379.

[23] Z. Shahryari, A. S. Goharrizi, and M. Azadi. 2010. Experimental Study of Methylene Blue Adsorption from Aqueous Solutions onto Carbon Nano Tubes. *Int. J. of Water Resources and Environmental Eng.* 2(2): 16-28.

[24] W. Zhou. 2016. A TiO_2 Embedded Structure for Perovskite Solar Cells with Anomalous Grain Growth and Effective Electron Extraction. *J. Mater. Chem.* 5(4): 1406-1414

[25] K. Fischer, R. Gläser, and A. Schulze. 2014. Nanoneedle and Nanotubular Titanium Dioxide – PES Mixed Matrix Membrane for Photocatalysis. *Appl. Catal. B Environ.* 160: 456-464.

[26] C. Yang, W. Dong, G. Cui, Y. Zhao, X. Shi, X. Xia, B. Tang and W. Wang. 2017. Highly Efficient Photocatalytic Degradation of Methylene Blue by P2ABSA-Modified TiO2 Nanocomposite Due to the Photosensitization Synergetic Effect of TiO2 and P2ABSA. *RSC Advance.* 7: 23699-23708.

[27] Z. A. M. Hir, P. Moradihamedani, A. H. Abdullah, and M. A. Mohamed. 2017. Immobilization of TiO2into Polyethersulfone Matrix as Hybrid Film Photocatalyst for Effective Degradation of Methyl Orange Dye. *Mater. Sci. Semicond. Process*. 57: 157-165.

[28] F. Chen, Z. Liu, Y. Liu, P. Fang, and Y. Dai. 2013. Enhanced Adsorption and Photocatalytic Degradation of High-Concentration Methylene Blue on Ag₂O-modified TiO₂-based Nanosheet. *Chem. Eng. J*. 221: 283-291

[29] F. J. Zhang, M. L. Chen, and W. C. Oh. 2010. Photoelectrocatalytic Properties of Ag-CNT/TiO₂ Composite Electrodes for Methylene Blue Degradation. *Xinxing Tan Cailiao/New Carbon Mater*. 25: 348-356.